Eur Biophys J (1993) 22:341–350

European Biophysics Journal
© Springer-Verlag 1993

Two components of the receptor current are developed from distinct elementary signals in *Limulus* ventral nerve photoreceptor

Károly Nagy, Klaus Contzen, Hennig Stieve

Institut für Biologie II, RWTH Aachen, Kopernikusstrasse 16, D-52074 Aachen, Germany

Received: 13 April 1993 / Accepted in revised form: 14 July 1993

Abstract. Transient elementary currents, bumps, stimulated by short dim light flashes were measured in ventral nerve photoreceptors of *Limulus*. It is demonstrated that light activates two types of bumps, which form two distinct components of the receptor current at higher light intensities. The two bump types, which are both assumed to be activated by single absorbed photons, differ in current amplitude and kinetic parameters. The current amplitude of one bump type is smaller than 0.3 nA and that of the other type is in the usual current range of up to several nanoamperes. The average latency of small bumps measured from the short stimulus flash is shorter than that of the large bumps. The small bumps have slower activation kinetics than the large bumps. It is demonstrated that with increasing flash intensity the small bumps overlap first and form a macroscopic current, on top of which the large bumps are superimposed. Results indicate that a single absorbed photon selectively activates only one kind of the enzyme cascades evoking one bump type. We conclude that the active meta conformation of a rhodopsin molecule selectively binds a specific type of G-protein, which is involved in the stimulation of one of the transduction cascades. The two bump types, which are the elements of two macroscopic current components support the previous assumption that light activates different transduction mechanisms in *Limulus* photoreceptors.

Key words: *Limulus* photoreceptor – Light-induced current – Single photon response – Bump types – Current components

Introduction

In most photoreceptor cells of invertebrates a single absorbed photon elicits a measurable transient electrical signal, a so-called bump (Yeandle 1958; Fuortes and Yeandle 1964; Dodge et al. 1968; Stieve 1986; Nagy 1991). The number of stochastically activated bumps increases with increasing stimulus intensity. Above a certain light intensity bumps overlap in time and form a macroscopic receptor potential or, under voltage clamp, a receptor current. Therefore, bumps are elements of the macroscopic electrical signals. They reflect the operation of elementary processes and thus are very important subjects for the study of the molecular mechanism of phototransduction.

Bumps have been investigated extensively (Fuortes and Yeandle 1964; Borselino and Fuortes 1968; Dodge et al. 1968; Wong et al. 1980; Keiper et al. 1984; Stieve 1986; Stieve et al. 1991). The usually observed current amplitude of a bump is some nanoamperes, the duration at the half-amplitude is 40 to 80 ms. The macroscopic receptor current could be reconstructed from bumps (Stieve et al. 1986) by disregarding some kinetic parameters which are changed by the stimulus intensity (for discussions see Nagy 1991).

The discovery of different light-activated receptor current components and single channel types in several photoreceptor cells of invertebrates (Maaz et al. 1981; Nagy 1990; Nagy and Stieve 1990; Deckert et al. 1992; Nasi 1991; Nasi and Gomez 1992; Hardie and Minke 1992) opens some new questions concerning the activation mechanism of bumps and the development of the current components from bumps. Since the existence of different light-activated processes is clearly supported by recent results (Deckert et al. 1992; Nagy 1993), we need to find out whether all processes contribute to the formation of a single bump or if one bump is due to the selective activation of one specific process. In the first case, one absorbed photon would activate two or more enzyme cascades and ion channel types evoking a uniform bump. In the second case, an excited rhodopsin would selectively activate only one enzyme cascade, resulting in as many bump types as current components.

The aim of the present work is to study this question in the ventral nerve photoreceptor of *Limulus*. It is shown that light activates two different types of elementary sig-

Correspondence to: K. Nagy

nals which form two components of the receptor current. This suggests that an excited rhodopsin selectively binds a certain type of G-protein activating one distinct enzyme cascade. Results support the previous observations and hypothesis (Nagy 1991, 1993; Deckert et al. 1992; Stieve and Benner 1992; Stieve et al. 1992) that light activates different transduction cascades and transmitters in this preparation.

Some parts of the results have been published in a preliminary form (Contzen et al. 1992; Nagy et al. 1992).

Materials and methods

The ventral nerves of *Limulus* were prepared in the usual way described earlier (Nagy 1990; Deckert et al. 1992). A two-electrode voltage clamp amplifier (npi electronic, Germany) was used to measure the receptor current. The physiological saline contained (in mM): 486 NaCl, 10 KCl, 25 $MgCl_2$, 30 $MgSO_4$, 10 $CaCl_2$, 10 HEPES and the pH was adjusted to 7.5 by NaOH. Intracellular electrodes having a resistance of 12 to 18 MΩ were filled with 1.0 M KCl. The experiments were carried out at 15°C, kept constant by Peltier-elements.

The photoreceptor cells were stimulated with a photo flash (Metz Mecablitz 60 ct-1, half-width <1 ms at the used intensities). An interference (Schott 540 ± 40 nm) and neutral density filters were placed in front of the light source. Cells were repetitively stimulated every 40 to 70 s. The stimulus intensities are given in the figure captions. The constant holding potential (V_h) was set close to the cell's dark potential, which was between -50 and -70 mV. 13 cells were used for the present study.

Experiments were carried out online with an IBM-compatible personal computer and an A/D-converter (Keithley DAS 16; for details see Nagy 1990). The currents were filtered at 120 to 150 Hz by a four pole Bessel filter and sampled at 1 kHz. The computer was used for further analyses of the currents. Parameters of bumps were determined by a program developed by H. Reuß (Reuß 1991). In some cases currents were digitally filtered before the analyses at 45 Hz by a low-pass filter of Bessel characteristics. Detailed analysis indicates changes $< 6\%$ in the mean values of parameters of bumps after this procedure (Reuß 1991).

Results

Figure 1 A demonstrates consecutive current traces after short dim flashes. Setting the flash intensity low, several current records appear empty, but others contain one or two bumps. In this example the average number of bumps per flash was 0.7. Bumps have current amplitudes larger than about 0.3 nA, similar to the values reported earlier (Stieve 1986; Stieve et al. 1991; Reuß 1991; Reuß and Stieve 1992). Averaging the current records containing bumps gave trace 1 in Fig. 1 B. This mean current has a latency of about 130 ms (marked by the dark arrow head), a time to maximum of about 300 ms (both measured from the flash), a current maximum of about 0.4 nA, a faster

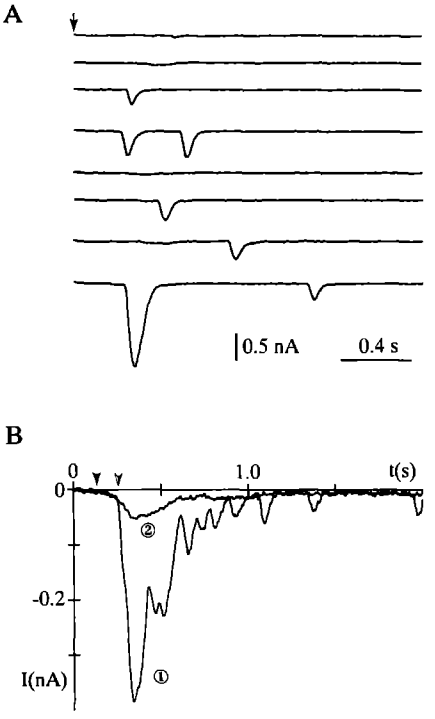

Fig. 1. **A** Consecutive current responses recorded in *Limulus* ventral nerve photoreceptor after short flashes applied at the arrow for each trace. Flashes occasionally activate bumps with different amplitude and latency. A green flash (7.2×10^7 photons/cm^2) was repeated every 50 s. **B** Averaged currents from traces having (1) and having no detectable bumps (2). Surprisingly trace 2 from "empty" records also indicates a light-activated inward current. Note that the traces overlap for times shorter than about 250 ms. The latency of both current increases was about 130 ms indicated by the dark arrow head. The half-open arrow head marks the time (≈ 250 ms) of the latency of the rapid current increase on trace 1. In each case 17 records were averaged. The holding potential was -50 mV

increasing and a slower decreasing phase. The averaged current is similar to the macroscopic current activated by intense flashes, but its kinetics are slower owing to the lower stimulus intensity (Stieve and Bruns 1980, 1983; Stieve et al. 1986, 1991).

Trace 2 in Fig. 1 B was obtained by averaging the "empty" records. This mean current surprisingly indicates a definite inward current with a latency of about 130 ms and a maximum of about 0.05 nA. The current decays slowly, but does not reach the dark current level in the 2 s recording time. The latency (about 130 ms) and the time to maximum (about 300 ms) of this trace are very close to those of trace 1, suggesting that trace 2 is a light-stimulated current. Thus we could conclude that the hardly visible deviations from the zero current on the "empty" traces in Fig. 1 A are not due to statistical noise or to an unstable background current, but are due to light-activated currents.

If the small current deflections are activated by light, one might assume (by analogy with the development of the usual bumps) that they are due to a certain type of single bump or to overlapping bumps which remained unresolved. This conclusion is plausible, because small bumps of shapes other than the usual ones have been reported recently for the ventral nerve photoreceptor of

Limulus (Reuß and Stieve 1992). Indeed, in nine cells from the thirteen used for the present investigation, we were able to find experimental conditions to resolve single small bumps. Some examples are shown in Fig. 2 A and B.

To observe small bumps it was necessary to set: *1)* the stimulus cycle longer than 40 s, *2)* the flash intensity to activate only few large bumps (<3 per flash on average) and *3)* the membrane potential more negative than -50 mV. The intensity of the flash and the stimulus cycle had to be matched for each cell individually. In four cells the conditions could not be set for recording single small bumps, because either the relative occurrence of the small bumps was low and with increasing flash intensity the large bumps superimposed on the small ones, or the signal to noise ratio was too low for the identification of the small bumps. (Note that the sizes of the usual bumps and the macroscopic currents also vary strongly from cell to cell; Stieve 1986; Deckert et al. 1992.)

For comparison of the usual and the small bumps Fig. 2 A shows selected current records. Some parts of the traces are plotted on enlarged scales in Fig. 2 B. These examples demonstrate single small and large bumps as well as superimposed small bumps. The shape of the small bumps is different from that of the large bumps. This is most clear if both bump types have a similar current amplitude (see e.g. trace 1 second part, trace 3 second part and trace 6 second part in Fig. 2 B). The small bumps are more rounded and have much slower kinetics than the large bumps. This difference can be used for the dinstinction of the responses to make a statistical analysis (see below).

At higher flash intensity single small bumps are hardly seen late after the flash (at $t>600$ ms), but more appear shortly after the flash. The shortened latency with increasing light intensity is consistent with earlier observations of the macroscopic and bump current; for a review see Nagy 1991. The early small bumps are often superimposed and form a pronounced current, similar to the mean of the "empty" traces demonstrated in Fig. 1 B. Such currents are shown in Fig. 3 A. On the early "macroscopic-like" small currents the large bumps are superimposed (Fig. 3 A). This is most clear if the large bumps have a longer latency than the time to maximum of the early small current.

The probability of finding traces without large bumps (see trace 4 in Fig. 3 A) is low at flash intensities which activate relatively large (≥ 0.2 nA) early currents. Collecting a large number of records, some such traces still appear (8 records from 200 in the example shown in Fig. 3 A), from which an averaged current can be calculated. This mean current is marked by C_1 in Fig. 3 B. From the records having large bumps a mean current was also calculated (trace C_2 in Fig. 3 B).

The two mean currents in Fig. 3 B precisely overlap in the early phase, at t less than about 250 ms, suggesting that *a)* traces with large bumps include the small early currents even if the small currents are not clearly visible (see Fig. 1 A and B) and *b)* the small currents and thus the small bumps have a shorter mean latency than the large bumps. Conclusion *a)* is supported by Fig. 1 B as well, where the averaged currents of "empty" and non-empty

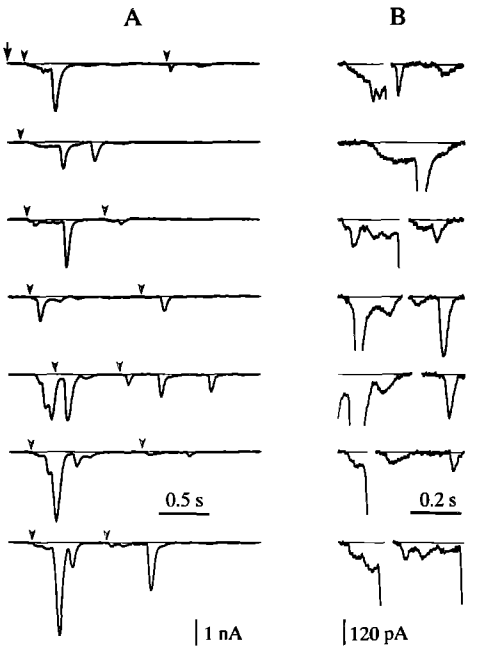

Fig. 2. A Current traces demonstrate light-activated small single and superimposed bumps as well as large bumps. Note that almost every large first bump is preceded by a slow current increase. A green flash (1.8×10^8 photons/cm^2) marked by the arrow stimulated the cell every 50 s. The holding potential was -60 mV. **B** Some ranges of current traces shown in A are plotted on enlarged scales (compare the calibration bars). The beginning of the selected ranges are marked by arrow heads in **A**. Currents demonstrate that the small events have a rounded shape, indicating slower kinetics than that of the large bumps

records overlap in the early phase, but there the effect is not so remarkable owing to the small amplitude of the mean current of "empty" records. The longer mean latency of large bumps can also be seen on trace 1 in Fig. 1 B. There the large rapid increase of the current at about 250 ms (marked by the half-open arrow head) indicates the latency of the large bumps, while the latency of the whole current at about 130 ms (marked by the dark arrow head) is due to the small unresolved bumps. Note that the latency of trace 1 is identical with the latency of the mean current of "empty" records in Fig. 1 B.

The different activation kinetics of the two bump types are clearly seen on the mean currents (Fig. 3 B). The time to maximum of the mean current of records with large bumps is about 580 ms and that of the traces without large bumps is about 350 ms. Consequently, the experiments with increased flash intensity show two important properties of the bump types: *a)* The small bumps are fused first to a macroscopic current while large single bumps are activated (Fig. 3 A), *b)* the small bumps have a faster activation mechanism than the large bumps (Fig. 3 B). These properties are similar to those of the macroscopic C_1 and C_2 components of the receptor current (Deckert et al. 1992; the abbreviations introduced previously are also used for the components here). For comparison, an example for the macroscopic C_1 and C_2 components is shown in Fig. 3 C. The increased flash intensity, used for the activation of these macroscopic currents, shortens the time scale and increases the current

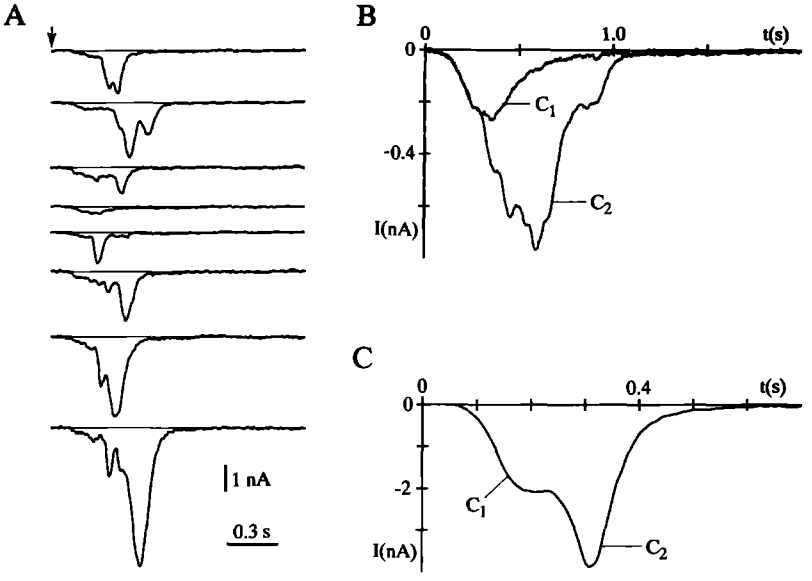

Fig. 3. A Light-activated currents show superimposed bumps of two types. The early current has a slow rising phase which is followed by fast increasing currents of large bumps. Note that on trace 4 there is no large bump. The flash (2.0×10^9 photons/cm^2) was repeated every 60 s and was applied at the arrow for each trace. The holding potential was -55 mV. **B** Averaged currents of traces without large bumps (C_1) and with large bumps (C_2). Note that the two traces completely overlap for time < 250 ms. **C** Macroscopic receptor current demonstrating the C_1 and C_2 components described previously (Deckert et al. 1992). Currents were evoked by a green flash (8.8×10^{10} photons/cm^2) applied at $t = 0$ s. The trace is the average of three responses measured in a different cell than those in **A**. The cell was stimulated every 120 s, the holding potential was -60 mV. The C_2 component is superimposed on the C_1 component in both **B** and **C**. Compare the different time and current scales in **B** and **C**

scale compared to Fig. 3 B. These are usual properties of the light-activated current (Stieve 1986; Stieve et al. 1986; Nagy 1991).

The macroscopic current components have been analysed recently (Deckert et al. 1992); therefore, only those properties which are important for the present discussion will be summarized here. The current components have different light sensitivities. At the lowest intensity only the C_1 component is activated, at higher intensity the C_1 and C_2 components are activated. With increasing intensity the C_1 component reaches a saturation size smaller than about 20 nA and the C_2 component increases up to several hundred nanoamperes (the current sizes are strongly cell specific). The latency of the C_2 component is more strongly shortened with increasing intensity than that of the C_1 component. Thus above a certain intensity the C_2 component completely overlaps the C_1 component (for details see Deckert et al. 1992). The current trace in Fig. 3 C was measured with moderate intensity for a clear temporal separation of the macroscopic C_1 and C_2. This current demonstrates that the C_2 component is superimposed on the C_1 component, as the mean current from records with large bumps is superimposed on the mean current from records without large bumps in Fig. 3 B. The different kinetics of the currents (latency and time to maximum) in Fig. 3 B, C are due to the different light-intensity. (Note that the bumps and macroscopic currents are activated on different time scales; Stieve 1986.)

Since the relative time parameters and the light-intensity dependences of the mean currents and the underlying bumps are similar to those of the macroscopic C_1 and C_2 current components, we suggest that the macroscopic C_1 component consists of the small early bumps and the macroscopic C_2 component of the large "usual" bumps. Consequently, we call the small bumps C_1 bumps and the large bumps C_2 bumps. Accordingly the mean currents of bumps are marked in Fig. 3 B.

Like the macroscopic current components (Nagy 1991; Deckert et al. 1992), the two bump types can only be observed under specific conditions. This is due to the following two reasons. First, the ratio of the activity of the large to small bumps is cell specific and thus varies strongly from cell to cell (compare Figs. 1 A, 2 A, 3 A and 4). Second, the difference in the mean latencies of bump types and the time to maximum of the averaged C_1 and C_2 currents (Fig. 3 B) are strongly dependent on the adaptation state of the cell and stimulus intensity, similar to that reported for the macroscopic C_1 and C_2 current components (Deckert et al. 1992). The best temporal separation of C_1 and C_2 bumps could be obtained with flash repetition rates longer than 40 s. This unusual long cycle time for bump measurements prolongs the latency of C_2 bumps more strongly than that of the C_1 bumps. A similar tendency for the separation of the macroscopic current components was observed with longer (> 4 min) cycle time (Deckert et al. 1992; Nagy 1993).

The best separation of the C_2 bumps from the macroscopic C_1 current is demonstrated in Fig. 4 for a cell, for

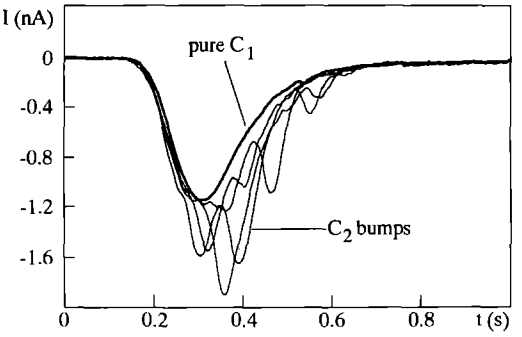

Fig. 4. An averaged current from traces which had only fused C_1 bumps, but no C_2 bumps (*thick line*) and single current traces having large C_2 bumps (*thin lines*). The single traces with C_2 bumps are superimposed on an envelope which is very close to the averaged current of the overlapping C_1 bumps. The single traces are similar to those shown in Fig. 3 A, but in this cell the size of the current from C_1 bumps is much larger. The saturated amplitude of the macroscopic C_2 component was also unusually large (1240 nA, not shown). The flash (2.2×10^9 photon/cm^2) applied at $t = 0$ s stimulated the cell every 70 s, the holding potential was -60 mV

which the conditions could be optimally set. With increasing light intensity the overlapping C_1 bumps fused first and formed a relatively large macroscopic C_1 component, on the top of which single C_2 bumps were observed (Fig. 4). The thick line in Fig. 4 shows the mean current of traces which did not have C_2 bumps in the selected time interval. The thin lines are single current traces clearly demonstrating C_2 bumps superimposed on the envelope of the C_1 component. The latencies of the pure C_1 and the single traces are about 135 ms. The pure C_1 reached a relatively large current maximum of about 1 nA, a value which is close to the range of that of the macroscopic C_1 component (2 to 20 nA; Deckert et al. 1992; Nagy 1993). The saturated size of the macroscopic C_2 component was 1240 nA in this cell, which is also large compared to the usual 300 to 600 nA (Deckert et al. 1992; Nagy 1993).

The discrimination of the C_1 bumps from the C_2 bumps is difficult. The C_1 bumps have a smaller current amplitude (about 50 to 300 pA; mean 153 pA $\pm$ 115 pA, $n = 844$ in 3 cells) than the C_2 bumps (the usual amplitude is larger than 500 pA; Stieve et al. 1991; Reuß and Stieve 1992). However, this criterion is not sufficient to allow discrimination, for the following reason. The amplitude histogram of the large usual bumps is best fit by an exponential function indicating that the usual bumps can also have amplitudes as small as the C_1 bumps. The only criterion for the distinction is the kinetics of the bumps. In most cases the kinetics of the rising phase of the current is quite different for the two bump types. As shown in Fig. 2A and B the C_1 bumps have a rounded shape with a slower rising phase than the C_2 bumps. This is quantitatively demonstrated in a cell (Fig. 5) in which a relatively large number of single small bumps were observed.

In Fig. 5 the distribution of the negative slope m of the linear fit to the rising phase of the current is shown for the first (open columns) and for the second bumps (dark columns; for definition of m see the inset in Fig. 5). Current traces with at least two bumps were taken for this calculation. We have found the selection of the first and the second bumps more adequate than an arbitrary decision after visual inspection, because mainly the C_1 bumps are activated first as the mean currents indicate in Fig. 3B. The histograms are significantly different for $m < 2$ pA/ms (Fig. 5). In this range the ratio of first bumps to the second ones is about 5 to 1. It follows that the mean slope is smaller for the first, i.e. for the C_1 bumps, than for the second, i.e. for the C_2 bumps (see the figure caption). The histograms overlap for $m > 2$ pA/ms indicating that the kinetics of the first and the second bumps are similar or, as is more probable, that there are no small bumps having such a large slope.

The moderate difference between the two histograms is probably due to the following reason. In several cases the second bump overlaps fully or partially the first bump. Then a C_2 bump is taken as a first bump. Furthermore, since the latency distributions of bumps are very wide (see below and Stieve and Bruns 1983; Stieve 1986) it may happen that a C_2 bump is activated first. In spite of the large overlapping of the histograms in Fig. 5 a criterion set for the kinetics resulted in a relatively good separation for the bump types shown below.

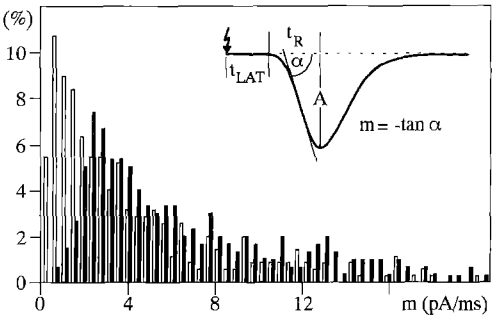

Fig. 5. Histograms for the slope m of the first (*open columns*) and the second bumps (*filled columns*). For the definition of m see the inset. The significant difference between the distribution for $m <$ about 2 pA/ms indicates that the first bumps, which are usually the C_1 bumps, have a slower rising kinetics than the second bumps, which are usually the C_2 bumps (see Figs. 2A and 3A). The mean slope m is 4.6 ± 4.8 pA/ms ($n = 345$) for the first and 6.8 ± 5.1 pA/ms ($n = 345$) for the second bumps. (Note that the large standard deviations are due to the exponentially decaying phase of the histograms.) The ratio of the number of the first to second bumps for $m < 2$ pA/ms is 4.8:1. The histograms are normalized to the number of events. The inset shows the definition of the latency t_{LAT} (measured from the begining of the flash), the rise time t_R, the slope m and the current amplitude

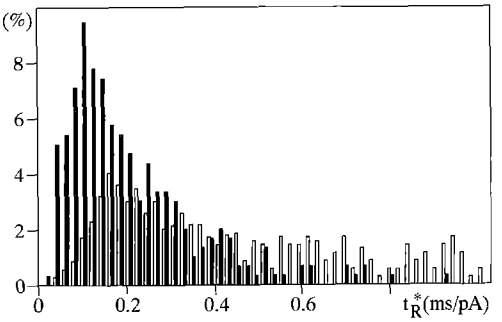

Fig. 6. Histograms for the normalized rise time t_R^* of the first (*open columns*) and the second bumps (*filled columns*) plotted with high resolution on expanded abscissa. The plot is from the same experiment as Fig. 5. The rise time t_R was normalized to the current amplitude A of the bump (for definition see the inset in Fig. 5). The mean of t_R^* is 0.62 ± 0.66 ms/pA ($n = 345$) for the first and 0.23 ± 0.25 ms/pA ($n = 345$) for the second bumps. The mean values indicate that the first bumps, usually the C_1 bumps, have slower normalized kinetics than the second, usually C_2 bumps. A threshold of 0.2 ms/pA for t_R^* was used later for the discrimination of the two bump sorts. The ratio of the number of the second to first bumps for $t_R^* < 0.2$ ms/pA is 3.9:1. The histograms are normalized to the number of events

The slope of the rising phase or the rise time of a bump (for definitions see the inset in Fig. 5) depends on the bump amplitude, because the larger the current the larger is the slope m and the longer is the rise time. Therefore, to sort the bumps we normalized the slope and the rise time to the amplitude of the bump. The histograms for the normalized rise time t_R^* are shown in Fig. 6 for the first and second bumps. A clear difference in the distribution can also be seen here for values < 0.2 ms/pA for the first and the second bumps. The first bumps, which are usually the smaller C_1 bumps, have larger normalized rise times

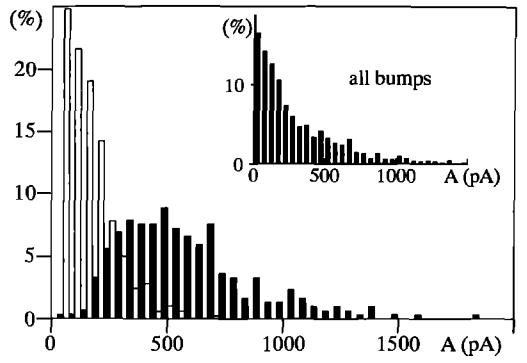

Fig. 7. Amplitude histograms constructed for bumps having a normalized rise time $t_R^* > 0.2$ ms/pA (*open columns*) and $t_R^* < 0.2$ ms/pA (*dark columns*). The mean amplitude is 132 ± 104 pA ($n = 500$) for the open columns (mainly C_1 bumps) and 562 ± 288 pA ($n = 305$) for the dark columns (mainly C_2 bumps; the same experiment as Fig. 5). The condition resulted in a clear distinction between the small and large bumps. Note that the condition for the selection is independent of the size of the bump. The inset shows the amplitude histograms of all bumps ($n = 805$). The histograms are normalized to the number of events

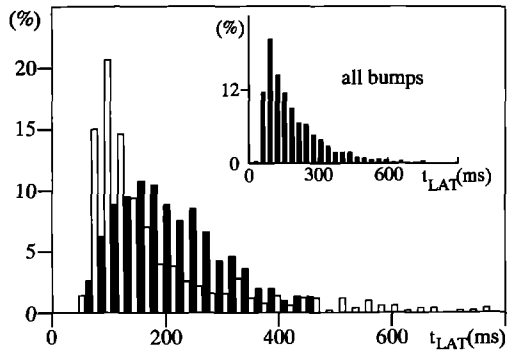

Fig. 8. Conditional latency histograms. *Open columns:* bumps having a normalized rise time $t_R^* > 0.2$ ms/pA, *dark columns:* bumps having a $t_R^* < 0.2$ ms/pA. The mean latency is 192 ± 176 ms ($n = 500$) for the open columns (mainly C_1 bumps) and 225 ± 89 ms ($n = 305$) for the dark columns (mainly C_2 bumps). The amplitude-independent selection criterion resulted in different distributions (the same experiment as Fig. 5). The histograms are normalized to the number of events

(mean 0.62 ms/pA) than the second, i.e. the large C_2 bumps (mean 0.23 ms/pA). Thus, for $t_R^* < 0.2$ ms/pA the relation of the number of the first to the second bumps is reversed compared to the distributions of absolute values (Fig. 5).

Setting a threshold criterion for the normalized rise time t_R^* the bumps can be sorted independently from the order of appearance. This calculation is important to sort all bumps (not only the first two bumps as above) and to show that by the normalized kinetic parameters the selection results in reasonable distributions for the small and large bumps. With a threshold of 0.2 ms/pA for the normalized rise time we constructed conditional amplitude and latency histograms (Fig. 7 und 8). The threshold was calculated from the histograms shown in Fig. 6 to have the largest ratio (about 1:4 for $t_R^* < 0.2$ ms/pA) for the number of the first to the second bumps. The condition resulted in clearly different amplitude histograms (Fig. 7).

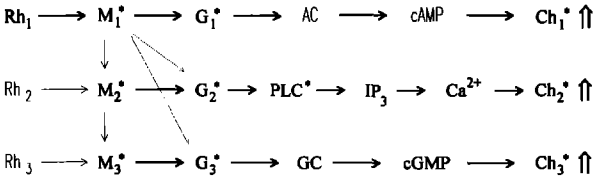

Fig. 9. Summary of models suggested for the selective activation of multiple transduction pathways in *Limulus* photoreceptor. The most probable states or substances are written in bold letters. For the selective activation of the two bump sorts and the three macroscopic current components (Deckert et al. 1992) three active meta conformations (M_i^*) of one or three rhodopsin molecules (Rh_i) and three G-proteins (G_i^*) are assumed. Three types of single channels (Ch_i) have also been observed (Nagy 1990; Nagy and Stieve 1990). Evidence for the IP_3-induced calcium release from intracellular stores has been published (Payne et al. 1986a, b, 1988; Frank and Fein 1991). This cascade activated the Ch_2 channels and the C_2 component (Nagy 1993). Two different cyclic nucleotides (probably cAMP, as well as cGMP) stimulate the C_1 and the C_3 components (Nagy 1993). AC indicates the adenylyl cyclase, GC the guanylyl cyclase. A simple hypothesis for the selective activation of the three mechanisms is to assume three types of rhodopsin molecules (Rh_i). The excited states are marked by asterisks. Upward open arrows indicate the opening of channels. For a sequential model with one excited rhodopsin molecule (Rh_1) transitions (thin downward arrows) between the active metarhodopsins M_i^* should be included. In this case the other rhodopsins (Rh_2 and Rh_3) should be disregarded. For further details see the text

The mean amplitude of bumps with $t_R^* > 0.2$ ms/pA is 132 pA (open columns in Fig. 7) and that of bumps with $t_R^* < 0.2$ ms/pA is 562 pA (dark columns in Fig. 7). These values support the subjective impression that the smaller C_1 bumps generally have slower rising kinetics and larger normalized rise time than the usual C_2 bumps. The successful separation of the small and large bumps indicates that the criterion set for the selection was quite appropriate. Similar results were obtained by setting a threshold for the normalized slope m^* for the selection.

The conditional latency histograms shown in Fig. 8 confirm that the small C_1 bumps have shorter latencies (mean 192 ms) than the larger C_2 bumps (mean 225 ms). This finding is to be expected, since the condition was obtained from the first and the second bumps. However, here all bumps were taken into account, as in Fig. 7. The conditional latency histograms overlap, but the form and the time to the maximum are clearly different. The time to the maximum is about 90 ms for bumps with $t_R^* > 0.2$ ms/pA (open columns; mainly C_1 bumps) and about 160 ms for bumps with $t_R^* < 0.2$ ms/pA (dark columns; mainly C_2 bumps). It is seen that several C_1 bumps are activated quite late after the flash as seen in Fig. 2. This property also suggests that the small bumps form the macroscopic C_1 component, because this component has a slower decaying phase than the C_2 component (see Figs. 4 and 9 in Deckert et al. 1992).

Discussion

The results presented demonstrate that light evokes two kinds of elementary currents (C_1 and C_2 bumps), which form two components of the macroscopic receptor cur-

rent in *Limulus* ventral nerve photoreceptor. The existence of another bump type (C_1) than the usual one (C_2) was demonstrated both by single bumps (Figs. 2 and 3 A) and by averaged currents in the case of unresolved signals (Fig. 1). In the latter case the mean current of "empty" records indicates a light-activated "background" current. The new bump type has a smaller amplitude (Figs. 2 and 7), a shorter latency (Figs. 3 and 8), slower activation kinetics (Figs. 5 and 6) and a higher light sensitivity (lower threshold) for activation than the usual bumps. These properties of the small bumps correlate with those observed for the macroscopic C_1 current component (Deckert et al. 1992). With increasing light intensity the overlapping small bumps first form a macroscopic current, on top of which the usual bumps are superimposed (Figs. 3 A and 4). The current component formed by the small overlapped bumps has a shorter time to maximum than that of the component formed by the usual large bumps (Fig. 3 B). On the basis of these properties the small and large bump sorts are identified as elements of the C_1 and C_2 components of the macroscopic receptor current, respectively.

A population of small bumps having different kinetic parameters than the usual bumps has been reported recently (Reuß 1991; Reuß and Stieve 1992). The current amplitude of those bumps was about 20 to 40 pA and their latency was 25–30% longer than that of the usual bumps. Those bumps were not identified as elements of any macroscopic current component. The parameters of the C_1 bumps calculated here cannot be directly compared to those reported by Reuß (1991) and Reuß and Stieve (1992), because Reuß and Stieve stimulated the cell every 10 s, in contrast to our stimulus cycle which was between 40 and 70 s. With the shorter stimulus cycle the condition of the cell is slightly different, a small steady-state "light adaptation" is caused, which is sufficient to change the parameters of the bumps (Stieve and Bruns 1980, 1983; Stieve et al. 1991).

Hypothetical models

On one hand, the classical theory of bump activation assumes that a bump is evoked by a single absorbed photon (Yeandle 1958; Fuortes and Yeandle 1964; Dodge et al. 1968; Wong et al. 1980). On the other hand, the light-activated current in *Limulus* ventral photoreceptor consists of three different components (Deckert et al. 1992), which have distinct adaptation and activation kinetics, light sensitivity as well as current-voltage characteristics and can be selectively inhibited by pharmacological means (Nagy 1993). It was concluded that the three current components are activated by three different mechanisms and transmitters. Therefore, the existence of clearly different bump types and the finding that they form distinct components of the receptor current suggest that one excited rhodopsin molecule elicits the release of only one of the three transmitter types.

For the selective transmitter release we discuss four hypothetical mechanisms. The models must explain, beside the properties of the bumps, the following properties of the macroscopic currents (Deckert et al. 1992): At low intensity one pathway, activating the C_1 component, is stimulated. At higher intensity two pathways are activated evoking the C_1 and the C_2 currents. The C_3 component is activated at even higher light intensity. The C_2 and C_3 components cannot be activated without the presence of the C_1.

Model A. There is one type of G-protein, which is activated by the meta conformation of one rhodopsin. This G-protein activates one enzyme cascade, the well established inositol phosphate cycle (Payne et al. 1988; Frank and Fein 1991; Hardie and Minke 1992), which is split into three branches at a late step. The pathways operate with certain probabilities depending on certain conditions (e.g. on the calcium concentration). The three different pathways produce different transmitters. The selective binding of one transmitter type by a channel type in the plasma membrane causes the opening of these channels and thus one of the three components of the receptor current.

Model B. One type of rhodopsin exists (Rh_1) with one meta conformation (M_1^*, Fig. 9), but there are three different G-protein types (G_i^*), each selectively activating an enzyme cascade. The binding of a G-protein type to M_1^* depends on specific conditions (e.g. on calcium concentration). A similar model containing three transduction pathways and transmitters was suggested earlier (Nagy 1990, 1991, 1993; Deckert et al. 1992; Stieve and Benner 1992; Reuß and Stieve 1992). However, in that model the selective activation was not considered.

Model C. One type of rhodopsin exists (Rh_1) with a sequence of different meta conformations (M_i^*), each of which selectively binds a G-protein type (G_i^*; Fig. 9). The active meta conformations have different lifetimes, which depend on certain conditions. Thus the conditions determine the probability of binding of a specific G-protein type resulting in the activation of one or the other pathway. This model has some common characteristic with the sequential models suggested earlier (Hamdorf and Razmjoo 1979; Lisman 1985; Levine et al. 1987), but those assumed one enzyme cascade.

Model D. Different types of rhodopsin molecules exist (as many types as G-protein types and transmitter types; Rh_i in Fig. 9), each with one meta conformation (M_i^*), which selectively bind a G-protein type (G_i^*). (The rhodopsin molecules would not necessarily have different absorption spectra, but would have different extinction coefficients.)

Model *A* seems to us improbable owing to the following reasons. *a)* Inhibitors of the inositol phosphate cycle do not block the light-activated current, but change its form (Frank and Fein 1991; Faddis and Brown 1993), indicating that beside the inositol phosphate cycle another enzyme cascade also operates in the cell (Nagy 1993). *b)* The latencies of the current components are different and depend differently on the adaptation state of the cell. For instance, the latency of C_1 remains constant and that

of the C_2 is shortened with progressive dark adaptation. No differenc in the latency of these components can be observed by an intense flash in a dark adapted cell. *c)* The distinct bump types cannot be explained by model *A* either (see below).

Models *B*, *C* and *D* can explain the macroscopic currents. For models, which need a switch to activate one or the other pathway, the early C_1 current could change the conditions to promote the activation of the latter currents (C_2 and C_3). However, these models could hardly be applied for the activation of the distinct bumps, since one bump can change the conditions only in a restricted area ($< 10\ \mu m^2$; Keiper et al. 1984; Tsuda 1987; Stieve and Schlösser 1989; Nagy 1991). Assuming that the photon absorption is statistically distributed (Fuortes and Yeandle 1964; Srebo and Behbehani 1972; Keiper et al. 1984) on the whole rhabdomeric surface of the cell (about $2 \times 10^5\ \mu m^2$, Calman and Chamberlain 1982), the probability is very low for the absorption a photon in the neighbourhood of another photon at low light intensity.

One could speculate that the transition probabilities from one pathway to the other depend on some local conditions, which are due to inhomogeneous distributions of ions, for instance. This possibility cannot be excluded. However, in this case the ratio of the (bump or macroscopic) C_1 and C_2 currents may not depend on the light intensity. In contrast, we observed a strong light-intensity dependence of the relative current amplitudes (Deckert et al. 1992).

Random binding of different G-proteins

For models *A*, *B* and *C* one could argue that the activation of two bump types can be explained by the random binding of two G-protein types. We find this hypothesis not probable owing to the following reasons. *a)* About 8 G-proteins participate in the activation of one bump (Kirkwood et al. 1989). Thus the stochastic binding of one or other G-protein type to the metarhodopsin would result in a uniform bump with a wide distribution of amplitudes and forms depending on the number of the bound G-protein types. The probability that 8 G-proteins of the same sort (to activate one bump type) are bound after each other to a metarhodopsin by chance is very low (3.9×10^{-3}). *b)* The uniform bumps (not two definite) would fuse to a macroscopic current, which would *not* consist of two components. In contrast, clear macroscopic C_1 and C_2 can be measured. *c)* Even if we assume that one G-protein activates one bump, random binding cannot work. Namely, in this case the ratio of the two currents would be independent of the light-intensity, contrary to the observations (Deckert et al. 1992).

For models which need a switch the most probable regulatory substance is calcium, since its concentration is increased by illumination (Bolsover and Brown 1985; Fein and Payne 1989; Payne et al. 1986 a, b; Stieve and Benner 1992). Therefore, the calcium concentration would be changed by the first, i.e. by the C_1 component and bump. However, the calcium concentration increase has a longer delay than the receptor current (Stieve and Benner 1992), because it is elicited by the activation of the C_2 current component (Nagy 1993) and thus by the C_2 bumps. It follows that either the C_1 bump and current changes the concentration of another substance, but not calcium, or models *A*, *B* and *C* cannot operate. Owing to the above arguments we find the hypothesis of more than one G-protein type probable and suggest that different types of rhodopsin molecules might exist in *Limulus* ventral nerve photoreceptor.

Components of multiple transduction pathways

Evidence for the following constituents of a transduction cascade consisting of two or three pathways have been demonstrated previously. *a)* G-proteins: Tsuda and Tsuda (1990) found two types, Robinson et al. (1990) three types of light-activated G-proteins in the photoreceptor cells of the squid. *b)* Ion channels: In ventral nerve photoreceptor of *Limulus* three light-activated current components (Deckert et al. 1992) and channel types (Nagy 1990; Nagy and Stieve 1990) were observed. Two channel types and macroscopic currents were reported for the photoreceptors of *Lima* (Nasi 1991), for the scallop *Pecten irradians* (Nasi and Gomez 1992) and for *Drosophila* (Hardie and Minke 1992). *c)* Enzyme cascades: In *Limulus* photoreceptor calcium chelators block the signal evoked by injection of calcium or inositol triphosphate (IP_3), but they do not block the light-evoked signal (Payne et al. 1986 a, b) indicating that light stimulates a calcium independent pathway as well. This conclusion is supported by recent results. Neomycin (an inhibitor of the IP_3 production) blocks the C_2 component and phosphodiesterase (which hydrolyses cGMP and cAMP) blocks the C_1 and C_3 components of the receptor current (Nagy 1993). Neomycin also inhibits the transient, but not the plateau phase of the receptor current stimulated by prolonged illumination (Frank and Fein 1991). High concentrations of neomycin did not block the receptor potential either, but changed the kinetics of the response (Faddis and Brown 1993). Thus, at least two processes are activated by light in the ventral nerve photoreceptor of *Limulus* as suggested earlier (Lisman and Brown 1971).

Conclusions from kinetical parameters

The different kinetics (latency and slope of the rising phase) of the bump types demonstrated here and that of the macroscopic current components (Deckert et al. 1992) indicate that the different enzyme cascades work with different rates. Furthermore, with increasing dark adaptation time the size of the macroscopic C_2 component increases and the latency and the time to maximum are strongly shortened (see Figs. 1 and 2 in Deckert et al. 1992). In contrast, the latency and time to maximum of C_1 and C_3 are constant in the course of dark adaptation (Deckert et al. 1992). Since the dark adaptation is regulated by the intracellular calcium concentration, the latency of C_2 must depend on the intracellular calcium concentration, in contrast to the latency of the C_1 and C_3 compo-

nents. This calcium-regulated kinetics of C_2 fits well to the model of the calcium inhibited calcium release (Payne et al. 1990), which was suggested recently to be responsible for the repetitive bump activation (Nagy 1992). It was assumed that the bumps appearing with a constant frequency form the second, i.e. the C_2 component of the receptor current. The presented results support this hypothesis, since it is shown that the C_2 component is developed from the usual bumps. C_2 is activated by the IP_3-induced calcium release (Nagy 1993), for which process a quantized mechanism was suggested by a transient calcium inhibition (Nagy 1992).

It was suggested that the C_1 and C_3 components (Nagy 1993) and thus the C_1 bumps are activated by cyclic nucleotides (C_1 possibly by cAMP). Since only the sizes, but not the kinetics of the macroscopic C_1 and C_3 components are changed with the adaptation state of the cell (Deckert et al. 1992) it is reasonable to assume that the kinetics of the cyclic nucleotide production are not much affected by the concentration change of calcium in the physiological range. This conclusion also suggests that transduction mechanisms with condition-dependent switchers are less probable.

Acknowledgements. We thank H. Reuß for providing us his computer program for bump analysis, H. Funk for the preparation, M. Rack, B. Huppertz and K.-H. Richter for stimulating discussions and reading the manuscript and the Deutsche Forschungsgemeinschaft for the financial support (Na 188/1-2). We are indebted to the reviewers of the Eur. Biophys. J. for the valuable comments on the manuscript.

References

Bolsover SR, Brown JE (1985) Calcium ion, an intracellular messenger of light adaptation, also participates in excitation of *Limulus* photoreceptors. J Physiol (London) 364:381–393

Borsellino A, Fuortes MGF (1968) Responses to single photons in visual cells of *Limulus*. J. Physiol (London) 196:507–539

Calman BG, Chamberlain SC (1982) Distinct lobes of *Limulus* ventral photoreceptors. II. Structure and ultrastructure. J Gen Physiol 80:839–862

Contzen K, Nagy K, Stieve H (1992) Quantum bumps that form two components of the light-activated current in *Limulus* photoreceptors. In: Elsner N, Richter DW (eds) Rhythmogenesis in neurons and networks. Georg Thieme Verlag, Stuttgart, New York, p 289

Deckert A, Nagy K, Helrich CS, Stieve H (1992) Three components in the light-induced current of the *Limulus* ventral photoreceptor. J Physiol (London) 453:69–96

Dodge FA, Knight BW, Toyoda J (1968) Voltage noise in *Limulus* visual cells. Science 160:88–90

Faddis MN, Brown JE (1993) Intracellular injection of heparin and polyamines. Effects on phototransduction in *Limulus* ventral photoreceptors. J Gen Physiol 101:909–931

Fein A, Payne R (1989) Phototransduction in *Limulus* photoreceptors: Roles of calcium and inositol trisphosphate. In: Stavenga DG, Hardie RC (eds) Facets of vision. Springer, Berlin Heidelberg New York, pp 173–185

Fuortes MGF, Yeandle S (1964) Probability of occurrence of discrete potential waves in the eye of *Limulus*. J Gen Physiol 47:443–463

Frank TM, Fein A (1991) The role of the inositol phosphate cascade in visual excitation of invertebrate microvillar photoreceptors. J Gen Physiol 97:697–723

Hamdorf K, Razmjoo S (1979) Photoconvertible pigment states and excitation in *Calliphora*; the induction and properties of the prolonged depolarising afterpotential. Biophys Struct Mechanism 5:137–161

Hardie RC, Minke B (1992) The *trp* gene is essential for a light-activated Ca^{2+} channel in *Drosophila* photoreceptors. Neuron 8: 643–651

Keiper W, Schnakenberg J, Stieve H (1984) Statistical analysis of quantum bump parameters in *Limulus* ventral photoreceptors. Z Naturforsch 39c:781–790

Kirkwood A, Weiner D, Lisman JE (1989) An estimate of the number of G regulatory proteins activated per excited rhodopsin in living *Limulus* ventral photoreceptors. Proc Natl Acad Sci, USA 86:3872–3876

Levine E, Crain E, Robinson P, Lisman J (1987) Nontransducing rhodopsin. J Gen Physiol 90:575–586

Lisman J (1985) The role of metarhodopsin in the generation of spontaneous quantum bumps in ultraviolet receptors of *Limulus* median eye. Evidence for reverse reactions into an active state. J Gen Physiol 85:171–187

Lisman JE, Brown JE (1971) Two light-induced processes in the photoreceptor cells of *Limulus* ventral eye. J Gen Physiol 58:544–561

Maaz G, Nagy K, Stieve H, Klomfaß J (1981) The electrical light response of the *Limulus* ventral nerve photoreceptor, a superposition of distinct components – observable by variation of the state of light adaptation. J Comp Physiol 141:303–310

Nagy K (1990) Kinetic properties of single ion channels activated by light in *Limulus* ventral nerve photoreceptors. Eur Biophys J 19:47–54

Nagy K (1991) Biophysical processes in invertebrate photoreceptors: recent progress and a critical overview based on *Limulus* photoreceptors. Q Rev Biophys 24:165–226

Nagy K (1992) Non-independent quantum bumps in *Limulus* ventral nerve photoreceptors – a new insight in the light transduction mechanism. Neurosci Lett 144:99–102

Nagy K (1993) Cyclic nucleotides and inositol trisphosphate activate distinct components of the receptor current in *Limulus* ventral nerve photoreceptors. Neurosci Lett 152:1–4

Nagy K, Stieve H (1990) Light-activated single channel currents in *Limulus* ventral photoreceptors. Eur Biophys J 18:221–224

Nagy K, Contzen K, Stieve H (1992) Different sorts of quantum bumps form two components of the receptor current in *Limulus* photoreceptors. Proceedings of The sensory systems and communications in arthropods. Hamburg (in press)

Nasi E (1991) Two light-dependent conductances in *Lima* rhabdomeric photoreceptors. J Gen Physiol 97:55–72

Nasi E, Gomes MP (1992) Light-activated ion channels in solitary photoreceptors of the scallop *Pecten irradians*. J Gen Physiol 99: 747–769

Payne R, Corson DW, Fein A (1986a) Pressure injection of calcium both excites and adapts *Limulus* ventral photoreceptors. J Gen Physiol 88:107–126

Payne R, Corson DW, Fein A, Berridge MJ (1986b) Excitation and adaptation of *Limulus* ventral nerve photoreceptors by inositol 1,4,5 trisphosphate result from a rise in intracellular calcium. J Gen Physiol 88:127–142

Payne R, Walz B, Levy S, Fein A (1988) The localization of calcium release by inositol trisphosphate in *Limulus* photoreceptors and its control by negative feedback. Philos Trans R Soc Lond Ser B 320:359–379

Payne R, Flores MF, Fein A (1990) Feedback inhibition by calcium limits the release of calcium by inositol triphosphate in *Limulus* ventral photoreceptors. Neuron 4:547–555

Reuß H (1991) Bumps, die elementaren Reizantworten der Photorezeptorzelle des *Limulus polyphemus*. Dissertation, RWTH Aachen

Reuß H, Stieve H (1992) Two different bump types of the ventral nerve photoreceptor of *Limulus*. Z Naturforsch 48c:92–95

Robinson PR, Wood SF, Szuts EZ, Fein A, Hamm HE, Lisman JE (1990) Light-dependent GTP-binding proteins in squid photoreceptors. Biochem J 272:79–85

Srebo R, Behbehani M (1972) Light adaptation of discrete waves in the *Limulus* photoreceptors. J Gen Physiol 60:86–101

Stieve H (1986) Bumps, the elementary excitatory responses of invertebrates. In: Stieve H (ed) The molecular mechanism of photoreception. Dahlem Konferenzen. Springer, Berlin Heidelberg New York, pp 199–230

Stieve H, Benner S (1992) The light-induced rise in cytosolic calcium starts later that the receptor current of *Limulus* ventral photoreceptor. Vision Res. 32:403–416

Stieve H, Bruns M (1980) Dependence of bump rate and bump size in *Limulus* ventral nerve photoreceptors on light adaptation and calcium concentration. Biophys Struct Mechanism 6:271–285

Stieve H, Bruns M (1983) Bump latency distribution and bump adaptation of *Limulus* ventral nerve photoreceptor in varied extracellular calcium concentration. Biophys Struct Mechanism 9:323–339

Stieve H, Schlösser B (1989) The light energy dependence of the *Limulus* photoreceptor current in two defined states of adaptation. Z Naturforsch 44c:999–1014

Stieve H, Schnakenberg J, Kuhn A, Reuss H (1986) An automatic gain control in the *Limulus* photoreceptor. In: Lüttgau HC (ed) Progress in Zoology, Vol 33. Membrane control of cellular activity. Gustav Fischer Verlag, Stuttgart, pp 367–376

Stieve H, Reuß H, Hennig HT, Klomfaß J (1991) Single photon evoked events of the ventral nerve photoreceptor cell of *Limulus*. Facilitation, adaptation and dependence on lowered external calcium. Z Naturforsch 46c:461–486

Stieve H, Niemeyer B, Aktories K, Hamm HE (1992) Disturbing GTP-binding protein function through microinjection into the visual cell of *Limulus*. Z Naturforsch 47c:915–921

Tsuda M (1987) Photoreception and phototransduction in invertebrate photoreceptors. Photochem Photobiol 45:915–931

Tsuda M, Tsuda T (1990) Two distinct light regulated G-proteins in octopus photoreceptors. Biochim Biophys Acta 1052:204–210

Yeandle S (1958) Evidence of quantized slow potentials in the eye of *Limulus*. Am J Ophtalmol 46:82–87

Wong F, Knight BW, Dodge FA (1980) Dispersion of latencies in photoreceptors of *Limulus* and the adapting bump model. J Gen Physiol 76:517–537